

KOHSENOW

TECHNICAL REPORT NO. 16

NUCLEATE BOILING BUBBLE GROWTH AND DEPARTURE

BY

BOGUMIL E. STANISZEWSKI

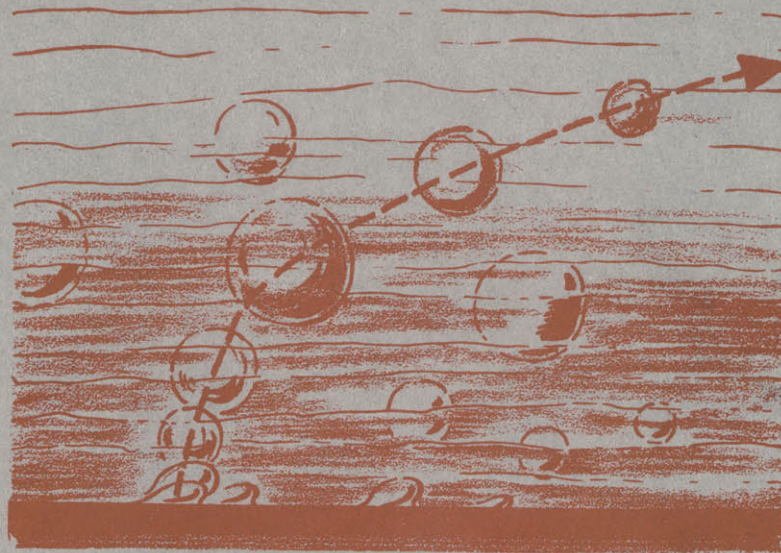
FOR

THE OFFICE OF NAVAL RESEARCH

NONR-1841(39)

DSR PROJECT NO. 7-7673

AUGUST 1959



DIVISION OF SPONSORED RESEARCH
MASSACHUSETTS INSTITUTE OF TECHNOLOGY
CAMBRIDGE, MASSACHUSETTS



Room 14-0551
77 Massachusetts Avenue
Cambridge, MA 02139
Ph: 617.253.5668 Fax: 617.253.1690
Email: docs@mit.edu
<http://libraries.mit.edu/docs>

DISCLAIMER OF QUALITY

Due to the condition of the original material, there are unavoidable flaws in this reproduction. We have made every effort possible to provide you with the best copy available. If you are dissatisfied with this product and find it unusable, please contact Document Services as soon as possible.

Thank you.

Due to the poor quality of the original document, there is some spotting or background shading in this document.

ABSTRACT

The vapor bubble formation on the heating surface during pool boiling has been studied experimentally. Experiments were made at the atmospheric pressure 28 psi and 40 psi, using degassed distilled water and ethanol.

The heat fluxes and heating surface temperatures have been measured simultaneously by taking high speed motion pictures of growing bubbles.

The diameter time curves of the bubbles and their diameter at the departure moment were obtained in these investigations. Bubble growth rates and bubble departure sizes have been compared to existing theories. It has been found that existing growth theories do not agree very well and that the departure size of the bubble is a function of the growth velocity.

Nucleate Boiling Bubble Growth and Departure

I. INTRODUCTION

The life of a bubble originating during nucleate pool boiling can be divided into three periods:

- a) formation of a small nucleus on heating surface
- b) growth of this small nucleus up to the moment of departure from the heating surface
- c) further growth of departed bubble during its passage through the layer of liquid above the heating surface.

The purpose of this work is to investigate the period b) with particular attention being paid to the circumstances of bubble departure.

The problem of bubble growth rate has been studied by a number of investigators. Plesset and Zwick (1), and Forster and Zuber (2) solved this problem theoretically in the case of a bubble growing in an infinite isothermal medium. Griffith (3), in his solution, took into consideration the non-isothermal temperature profile around the growing bubble. Bankoff (4), in his analysis, assumed the existence of a very thin liquid layer, with a certain temperature distribution, surrounding the growing bubble.

The experimental data taken on bubble growth rates are very incomplete and are concerned mainly with surface boiling (6), (7). A few papers devoted to pool boiling (8) contain a certain amount of information, but it has been obtained mostly at low heat fluxes and at the atmospheric pressure only. The lack of sufficient experimental data does not permit one to analyze and to check the bubble growth theories. Moreover, the observations of bubbles departing from the heating surface show that the present criterion of bubble departure is inadequate. The dynamics of growing bubbles seems to be a particularly important factor in influencing the diameter of a bubble as it departs from the heating surface.

In this situation it seems to be worthwhile to do a new investigation in order to determine the mechanism of growth and departure of bubbles. This is the objective of the present work.

II. EXPERIMENTAL METHODS

In this investigation, the diameter-time curves of the bubbles and their diameter at the departure moment were obtained by high speed motion pictures. At the same time, measurements were made of heat flux and surface temperature.

Two liquids were used in these experiments, distilled water and methyl alcohol. The heating surface was made of copper. The measurements have been made at three different pressures, atmospheric pressure, 28 psia, and 40 psia. The heat flux was varied at atmospheric pressure between 15% and 80% of burn-out heat flux $(q/A)_{\max}$, and at higher pressures it only reached about 35% of $(q/A)_{\max}$ because of difficulties in distinguishing the separate bubbles.

The position of the heating surface has been changed also; however, the majority of experiments have been made with the surface in a horizontal position. Two runs were performed with the heating surface vertically located in order to investigate the influence of the heater surface position. Moreover, in two experimental runs the height of liquid layer above the heating surface was as small as 8 diameters of detaching bubbles (about one inch).

The experimental apparatus is shown in Figures 1 and 2. Appendix I contains the exact description of apparatus construction and the details concerning the experimental technique. A brief description of the experiments is as follows.

Pictures of growing bubbles were taken by simultaneous measurements of heating power, temperatures of liquid in three different points, and heating surface temperature. The latter has been determined by extrapolation of temperature measurements taken at three points in the straight conductor section.

The boiling surface had the shape of a sphere section with large radius of curvature. It was equivalent to a plane surface of length 1", width 1/8". In order to eliminate edge effects, a very thin copper disc was attached to the upper heater surface and this disc was soft-soldered to the heater. The error caused by losses of heat conducted through the disc was very small because its thickness was only about 1% of heater width.

Pictures were taken with a high speed Wollensack camera coupled to a stroboscope lamp. The picture frequency was about 1200 frames per second which

was sufficient to obtain the bubble diameter time curves.

In addition to the measurements, a qualitative analysis of the films has been made in order to find any characteristic details which could be observed.

III. RESULTS

Observations made during the runs and the analysis of the films showed that the bubbles originated mostly at these same steady active sites. In general, no interruptions between successive bubbles were observed, but sometimes such breaks occurred. In addition, one also could observe intermittent pauses in activity of some active sites and periodical creation of new ones.

The results of measurement are presented in Figures 3 through 14 as curves $D = f(t)$. Successive bubbles are matched with numbers: 1, 2, etc. and were observed at different points on the heating surface. The corresponding curves give an idea of the difference in the bubble growth rates along the surface.

These curves are sometimes very different from each other. Because no systematic dependence of character of these curves on the nucleation place has been observed, these differences appear to be caused by the statistical character of the nucleation process. A good illustration of the statistical character of bubbles growing is shown in Figure 15 in which are presented the results of observations of one active site over a long period of time. The successive bubbles originating at one spot are numbered on the horizontal axis of this figure. The vertical axis in the upper half of the drawing is the diameter of detaching bubbles. In the lower half is a plot of the number, n , of frames from the creation to the departure which is inversely proportional to the bubble frequency versus the number of the bubble. The character of the bubble diameter and frequency curves is periodical, but not regular.

The comparison of curves obtained in different cases showed the following characteristics:

a) The bubble growth rate curves are almost independent of the heat flux but when the heat flux is high (about 80% of $(q/A)_{\max}$, Fig. 7), one can observe the increase of bubble departure diameter and the decrease of bubble frequency.

b) The decrease of the height of a liquid layer above the heating surface to the value of about 0.8" causes a small change in the bubble diameter-time

curves. As in the previous case, the bubble frequency decreases and the bubble departure diameter increases.

c) The comparison of bubble growth rate curves obtained from the experiments made with the heating surface in both the vertical and horizontal positions shows that the bubble departure diameter is approximately the same in both cases, but the bubble grows more slowly on the vertical surface.

d) The pressure increase causes a decrease in the bubble frequency and departure diameter. The slope of bubble diameter-time curve decreases also with increasing pressure.

Afterwards it was observed that the number of active sites increases remarkably with a pressure increase.

There is another important and interesting phenomenon occurring during boiling, namely bubble agglomeration. There are two different ways in which this agglomeration occurs. The first one is the overtaking of a bubble, which has been detached previously, by a new bubble growing on the heater surface. The other way is the joining of neighboring bubbles growing on the heating surface to form one greater bubble which afterwards departs.

The first manner of agglomeration takes place rather rarely but has been found even in small heat fluxes. The second one depends on the number of active sites. When this number is larger, which occurs at higher heat fluxes or higher pressures, then the joining of neighboring bubbles occurs more frequently. This last phenomenon is sometimes very regular in the sense that the agglomerated bubbles originating at the same place are similar to each other in frequency and diameter.

It was also possible to measure the contact angle in these pictures. This measurement showed that the contact angle did not depend on heat flux and was the same for both water and methyl alcohol. The value of this angle at atmospheric pressure was about 43° . An increase in pressure caused an insignificant increase of contact angle up to the values of about 45° at 28 psi and about 47° at 40 psi.

IV. DISCUSSION AND ANALYSIS OF THE DATA

Bubble Growth

The bubble diameter-time curves obtained permit comparison with the growth rate theories. According to the Plesset-Zwick, and Forster-Zuber theories, the functions $R = f(t)$ are:

$$\text{Plesset-Zwick:} \quad R = \left(\frac{12}{\pi}\right)^{1/2} \Delta T \left[\frac{\rho_l c_l}{h_{fg} \rho_v} a_t \cdot t \right]^{1/2} \quad (1)$$

$$\text{Forster-Zuber:} \quad R = \pi^{1/2} \Delta T \left[\frac{\rho_l c_l}{h_{fg} \rho_v} a_t \cdot t \right]^{1/2} \quad (2)$$

These formulas were obtained by the solution of the differential equations describing the heat transfer process between the growing bubble and surrounding liquid. Some simplifying assumptions were introduced in this analysis, the most important one being that the bubble is growing in an infinite volume of isothermal liquid.

Both formulas can be written in the form:

$$R = C \cdot \Delta T t^{1/2} \quad (3)$$

where the constant C contains also liquid and vapor physical properties, and for given liquid depends on pressure only.

According to equation (3), the curve $R = f(t)$ is a parabola whose shape depends on the temperature difference ΔT and liquid physical properties. Griffith solved this same problem, assuming the certain temperature distribution in the vicinity of the heating surface. Under this assumption, only the numerical solution could be given. The analysis of Griffith's $R = f(t)$ curves shows that they can be described by the equation of form:

$$R = C_o t^n \quad (4)$$

but n would vary with time t . In the early growth stage the value of n is close to $1/2$, then decreases up to 0.22 to 0.35 and is almost constant. The value of n in the later stage depends on liquid physical properties.

Bankoff gave the solution of the bubble growth rate problem under the assumption that the bubble is surrounded by a very thin liquid layer with a specified temperature distribution. The solution to the equations was accomplished by introducing a constant coefficient which was determined from experiments. Unfortunately, the value of this coefficient varied dependently on the experimental conditions.

The analysis of data obtained in experiments discussed in this report shows that if the curves $D = f(t)$ are presented in the form $D = c t^n$ then n will vary with time t . In general, n is bigger than $1/2$ in the early stage of bubble growth and sometimes reaches the value of 1. Afterwards, it decreases with time and in the late stage has, roughly, a value of about $1/3$.

These results indicate that the Plesset-Zwick and Forster-Zuber formulas do not agree well with actual experimental bubble growth on a heating surface in pool boiling. Griffith's solution agrees relatively well with experimental curves in the late growth stage, but in the early stage the actual growth is quicker. Bankoff's formula permits one to obtain the true shape of the bubble diameter time curve; however, it contains an empirical coefficient with an unidentified characteristic. Nevertheless, his assumption of existence of a thin liquid layer around the growing bubble seems to be reasonable because it provides agreement between the experimental bubble growth curve and the theoretical one.

Temperature Distribution in the Vicinity of the Heating Surface

The analysis of bubble growth rate curves shows that they do not change significantly with the changing of the heat flux. Since the shape of these curves depends on temperature distribution in the vicinity of the heating surface, it also can be expected that this distribution will not change very much with the heat flux. An increase in the heat flux, however, causes an increase in the heating surface temperature. The independence of the temperature dis-

tribution on heat flux can be explained by the fact that there is a temperature drop in a very thin layer at the heating surface up to the certain value which is independent of heat flux.

The approximate calculation based on the Forster-Zuber equation shows that in the first stage of bubble growth in the water at atmospheric pressure, the liquid temperature ought to be equal to 15°F above saturation temperature. Assuming that the heat is only conducted in the above-mentioned thin liquid layer and that the temperature drop in it is equal to 15°F, it is possible to compute the thickness of this layer. The results of these calculations based on experimental data are presented in Table 1.

Table 1

Heat flux, Btu/hr ft ²	Measured wall superheat, °F	Calculated liquid layer thickness, in.
5.5 · 10 ⁴	15.3	8.10 ⁻⁵
8.0 · 10 ⁴	21.6	4.10 ⁻⁴
1.1 · 10 ⁵	21.2	3.10 ⁻⁴
1.36 · 10 ⁵	25.7	3.3.10 ⁻⁴
1.82 · 10 ⁵	26.8	4.10 ⁻⁴
2.1 · 10 ⁵	28.8	3.3.10 ⁻⁴
2.94 · 10 ⁵	35	3.3.10 ⁻⁴

Although the calculated values of layer thicknesses are almost independent of heat flux, one might expect that they will decrease with the increase of heat flux. The calculations based on the well known formula:

$$q/A = C \Delta T^n$$

show that under the assumption of constant temperature drop equal to 15°F outside the thin layer, the thickness of this layer decreases from 5.34 · 10⁻⁴ to 3.8 · 10⁻⁴ inches when the heat flux increases from 7.2 · 10⁴ Btu/hr ft² to 2.86 · 10⁵ Btu/hr ft². These results show a certain similarity to the results of turbulent flow experiments in which the very small boundary layer thickness

is proportional to the 0.2 power of the Reynolds number. If the heat flux is treated as a value proportional to the Reynolds number, then the changing of boundary layer thickness is of the same order of magnitude as that observed in turbulent flow.

It is worthwhile to compare the boundary layer thickness with the dimension of nucleus, corresponding to the superheat $\Delta T = 15^\circ \text{F}$. The radius of such a nucleus for water at the atmospheric pressure according to the formula:

$$r^* = \frac{2\sigma T_s v_{fg}}{h_{fg} \Delta T}$$

is equal roughly to $1.6 \cdot 10^{-4}$ inch which is about 1/2 of the boundary layer thickness.

fD Product

The experiments which have been performed permit, also, the calculation of the values of product fD, which, according to Jakob, is constant for different liquids at the atmospheric pressure.

It can be shown that in the case when there is no interval between bubbles the product fD is equal to (see appendix II):

$$fD = a_t \frac{S_L C_p}{S_v h_{fg}} \frac{1}{\psi(R)} \quad (5)$$

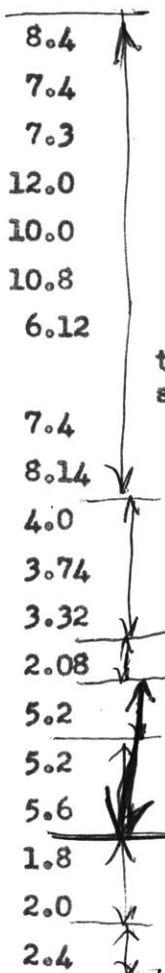
where $\psi(R)$ is the surface-time average value of bubble wall temperature gradient.

The form of equation (5) suggests that fD will differ with variations in physical properties and temperature gradients and does not have to be constant for different liquids. Moreover, one can expect that this product also will vary with changing pressure.

The calculations made on the basis of the present data show that the product fD is almost independent of heat flux for its moderate values. It in-

creases when the heat flux approaches its burnout value and it decreases when the pressure increases. Furthermore, the fD products are different for water and for methyl alcohol. The average values of fD are presented in Table II.

Table II

Liquid	Heat Flux q/A Btu/hr sq ft	fD_h $\sqrt{\frac{0.99(P_L - P_v)}{P_L^2}}$	Pressure	fD inch/sec	Remarks
water	$1.36 \cdot 10^5$	1.3691	atmospheric	8.4	 <p>Vertical position of heating surface</p>
"	$8 \cdot 10^4$	1.2061	"	7.4	
"	$5.5 \cdot 10^4$	1.1898	"	7.3	
"	$2.94 \cdot 10^5$	1.9538	"	12.0	
"	$1.1 \cdot 10^5$	1.6298	"	10.0	
"	$1.82 \cdot 10^5$	1.7602	"	10.8	
"	$9.4 \cdot 10^4$	0.9975	"	6.12	
"	$7.5 \cdot 10^4$	1.2061	"	7.4	
"	$2.1 \cdot 10^5$	1.3267	"	8.14	
"	$5.7 \cdot 10^4$	0.6630	28 psi	4.0	
"	$1.09 \cdot 10^5$	0.6200	28 psi	3.74	
"	$6.1 \cdot 10^4$	0.5503	28 psi	3.32	
"	$7.2 \cdot 10^4$	0.3466	40 psi	2.08	
methyl alcohol	$7.9 \cdot 10^4$		atmospheric	5.2	
"	$3.5 \cdot 10^4$		"	5.2	
"	$5.1 \cdot 10^4$		"	5.6	
"	$3.5 \cdot 10^4$		28 psi	1.8	
"	$3.6 \cdot 10^4$		28 psi	2.0	
"	$3.7 \cdot 10^4$		40 psi	2.4	

Bubble Departure

W. Fritz (9) gave, on the basis of previous theoretical work, the formula for the diameter of bubbles detaching from the heating surface:

$$D = 0.0119 \beta \sqrt{\frac{2\sigma}{g(\rho_l - \rho_v)}} \quad (6)$$

This formula was obtained from a balance of gravity and surface tension forces acting on the bubble attached to the heater surface. The value of the constant coefficient was fixed on the basis of experimental data.

The analysis of the bubble growth rate curves shows that the bubble diameters at the departure moment vary within very large limits. Deviations of measured diameters and the values calculated from Fritz's formula are much larger than presented by Jakob (10) in his book. These differences are particularly great at higher pressures.

Furthermore, it has been observed that the bubbles growing more quickly attain bigger departure diameters and vice versa. This observation permits an assumption to be made that bubble growth velocity influences the departing bubble diameter. Such an influence could also be caused by the action of other forces, such as inertia and drag, which depend on bubble growth velocity. These forces have not been taken into account in the Fritz analysis.

From the experimental data, it is possible to correlate the velocity of bubble growth in the last stage and the departure diameter. This correlation is as follows:

$$D = D_0 + a \frac{dD}{dt} \quad (7)$$

where D_0 is the bubble diameter when the bubble growth velocity $\frac{dD}{dt} = 0$. The value of D_0 was found by extrapolation of a straight line, defined by the equation (7), up to the point of intersection with D axis. They are equal correspondingly:

for water	$D_o = 0.048''$
for methyl alcohol	$D_o = 0.028''$

The bubble departure diameters calculated for the Fritz equation at the experimental conditions, are almost independent of pressure. The reason for this fact is that the influence of changes in the surface tension and the liquid and vapor densities is compensated by increase of contact angle. These calculated values are

for water	0.078''
for methyl alcohol	0.047''

The ratio of D_o based on present experimental data and the value calculated from the Fritz formula is the same for these liquids and is equal to 0.6. That is, the bubbles depart at a smaller size than one would expect from their contact angles. Furthermore, the general correlation has been found in the form:

$$\frac{D}{D_o} = 1 + 0.435 \frac{dD}{dt} \quad (8)$$

or

$$D = 0.0071 \sqrt{\frac{2\sigma}{g(\rho_l - \rho_v)}} \left(1 + 0.435 \frac{dD}{dt}\right)$$

in which dD/dt is given in inches per second.

This formula correlates all data obtained for both liquids in the entire range of heat fluxes and pressures. The comparison of the experimental data with equation (8) is presented in Figure 16. The dotted lines correspond to the $\pm 25\%$ deviations from the values determined by equation (8) and are represented by the straight line.

It is worthwhile to emphasize that, because of water circulation in the vicinity of the bubbles, the relative bubble wall velocity can differ from the

value of $\frac{dD}{dt}$. This difference could also induce the deviations of experimental data. Afterwards, it can be stated that the mean values of bubble departure diameters measured at atmospheric pressure agreed well with the Fritz formula.

V. CONCLUSIONS

1. The bubble growth rate curves are almost independent of the heat flux in the range between 10% and 60% of burnout heat flux.
2. The pressure increase causes decrease of bubble frequency and diameter. The slope of the bubble diameter-time curve decreases also.
3. The number of active sites increases remarkably with a pressure increase.
4. The slope of the bubble diameter-time curves in the early stage of bubble growth is steeper than those corresponding to the previous theories.
5. The fD_b product depends on pressure and decreases when the pressure increases. Moreover, the comparison of fD_b values for water and methyl alcohol shows that they are not equal.
6. Bubble departure diameters depend on the growth velocity in the last stage. The diameters measured at the atmospheric pressure and moderate heat flux values agree with the Fritz-Jakob formula.

VI. ACKNOWLEDGMENT

Publication costs for this work have been supplied by the ONR. The work was performed in the Heat Transfer Laboratory of the Massachusetts Institute of Technology which is under the direction of Professor Warren M. Rohsenow.

I am very grateful to Professors Rohsenow and Griffith for this opportunity to work with them in the Heat Transfer Laboratory and for their help and suggestions throughout the past year.

APPENDIX I

A) Description of the Apparatus and Experimental Methods

The experimental set-up is shown in Figure 1. The test boiler was made of stainless steel. Observation windows were fixed to two side flanges of the test boiler. The windows were made of temperature and pressure resistant glass panels of one inch diameter, placed in stainless steel frames and sealed with O-rings. The windows were recessed to reduce heat losses and to make sure that the liquid close to the glass panels was not subcooled.

The cooling coil, pressure gage, safety valve and three thermocouples for liquid temperature measurement are fixed to the upper flange. The cooling coil, which was made of copper tubing, was connected with a water container held at fixed temperature and pressure. A throttling valve was used to adjust the rate of cooling. The pressure gage was fixed to a tube to which the safety valve was attached also. The filling of the test boiler with fluid was performed through the safety valve.

The three chromel-constantan thermocouples of #30 wire were used to measure the temperature of the liquid. They were fixed at the following distances above the heating surface: 0.5", 1.5" and 3".

The boiling unit shown in Fig. 2 was constructed with a copper collector section to which the heat was supplied by a 160 watt Chromalox electrical heater. The heater is connected to A.C. line through a wattmeter and an adjustable rheostat. The heat is then passed through a straight conductor to a 1" long, 1/8" wide, slightly curved surface. This surface had a .006" thick copper disc soft-soldered to it. The boiling takes place along the 1" x 1/8" strip. The thickness of the copper disc was so small that conduction heat losses were insignificant. This unit was fixed inside a stainless steel tube attached to the bottom of the boiler unit. The air gap between the collector and the tube provided heat insulation. The upper part of the tube connected with the top of the test boiler was a vapor filled compartment. This acted as a pressure balance and heat insulator. In the straight conductor part of the boiling unit were imbedded three chromel-constantan #30 wire thermocouples. The distances from the boiling surface to the thermocouple junctions were: 1/64", 23/64" and 45/64".

The readings from these thermocouples were extrapolated to give the surface temperatures with good approximation. The thermocouple leads were inside small diameter stainless steel tubes with special seals at the outer end. A thermos bottle was used for the cold ends of the thermocouples, which were connected with a potentiometer through a six-way switch.

A drain valve was also attached to the bottom of the test boiler. To heat up the liquid and to maintain it at a constant temperature, the whole test boiler was surrounded by two heating coils fed with A.C. through two regulated variacs. The whole experimental assembly was covered by an insulation.

B) The Experimental Technique

Before each run the heating surface was carefully cleaned. The same surface roughness was maintained during the whole set of experiments by finishing the boiling surface with 2/0 emery cloth.

The test apparatus was filled with degassed liquid. The liquid was then heated, using the boiling unit heater and heating coils. After reaching the boiling temperature, the liquid was permitted to get rid of the gas remnants for about one hour before starting the tests. The desired heat flux value was then adjusted and, after reaching steady state conditions, measurements were recorded. These conditions were very carefully checked during each run, to make sure that no deviations from the steady state occurred. Particular attention was paid to the temperature readings.

During each run the following measurements were made: heat power, liquid temperatures, boiling unit temperatures. High speed photographs were taken with a Wollensack camera using stroboscopic lighting. Four instrument readings were taken at each run and the average values were used for evaluation purposes.

A Kodak Tri-X negative 50' film for high speed photography was used. About 1200 frames per second were taken, which necessitated a reduction of the voltage supplied to the Wollensack camera motors to about 40 volts. The "Goose" unit was used to control the camera operation. The camera runs were of 2.5 sec. duration and the timers were set on position: camera 2.6--event 1.2. The four-way switch was on position 3. For such switch and timer setting, the strobe lamp was switched on 1.2 sec. after the camera-motor started running; hence, the first half of the film was unexposed. This permitted the use of the same film twice by mounting it to run in opposite directions.

The stroboscope lamp was aligned with the window axis and placed as close as possible to the window. To provide a uniformly scattered lighting, a thin piece of waxed paper was placed between the lamp and window. To obtain the proper exposure, the stroboscope lamp condenser was in the .04MFD position. Such a setting allows the safe use of the strobe lamp. The photographs were then taken with an F/2 opening. The camera was placed as close as possible to the test section without losing the sharp focus required. Kodak Microdol developer was used and the developing time was thirty minutes, the fixing time twenty minutes.

The bubble diameter measurements were made using a microfilm projector. The picture magnification was obtained by using the window diameter as a reference length, and applying a correction due to the difference in distances between the bubble formation plane, window plane and focus of the camera lens. The frame frequency was determined by reference to the 1/20 sec reference timing marks on the film.

It should be noted that it was necessary to introduce a correction to determine the heat flux. The effective amount of heat transmitted per unit time to the liquid was lower than the electric power indicated by the wattmeter. This was caused by heat losses due to convection and conduction between the copper heat collector and its surroundings. To determine the heat losses, measurements were first made at a temperature close to but below the liquid boiling temperature. The heat transferred to the liquid through the boiling surface was then calculated, using the natural convection formula. This agreed with the calculated heat conducted through the straight conductor, assuming that the steady state heat flow is reached and that there are no heat losses to the surroundings of this part. These last calculations were based on thermocouple readings. The efficiency of the boiling unit is thus determined as about 75% and is almost independent of the heat flux.

APPENDIX II

A) The Derivation of a Formula for τ_D

The amount of heat transferred by the bubble wall during the time dt is equal to

$$q = -k \int_A \left(\frac{\partial T}{\partial r} \right)_{r=R} dA = -k \overline{\text{grad}_r T} A \quad (a)$$

On the other hand, from the first law of thermodynamics,

$$q = 4\pi R^2 \rho_v h_{fg} \frac{dR}{dt} \quad (b)$$

These two values have to be equal; therefore,

$$4\pi R^2 \rho_v h_{fg} \frac{dR}{dt} = -k \overline{\text{grad}_r T} A = -k \overline{\text{grad}_r T} 4\pi R^2$$

and

$$\frac{dR}{dt} = - \frac{k}{\rho_v h_{fg}} \overline{\text{grad}_r T}$$

Introducing the thermal diffusivity $a_t = \frac{k}{\rho_l c}$ will be

$$\frac{dR}{dt} = - a_t \frac{\rho_l c}{\rho_v h_{fg}} \overline{\text{grad}_r T} \quad (c)$$

when the notation $-\overline{\text{grad}_r T} = \phi(R)$ is introduced

(because $-\overline{\text{grad}_r T}$ is a function of time and of R also.)

Then, including this notation in equation (c), one obtains

$$\frac{dR}{\phi(R)} = a_t \frac{\rho_l c}{\rho_v h_{fg}} dt \quad (d)$$

The integration of equation (d) gives the result

$$D \cdot \psi(R) = \int_0^R \frac{dR}{\psi(R)} = a_t \frac{\rho_l c}{\rho_v h_{fg}} \int_0^{t_0} dt$$

where t_0 is the time from the bubble initiation to departure.
However,

$$\int_0^{t_0} dt = t_0$$

Therefore, when there is no interval between bubbles, $t_0 = 1/f$ which is the reciprocal value of bubble frequency,

$$fD = a_t \frac{\rho_l c}{\rho_v h_{fg}} \frac{1}{\psi(R)} \quad (e)$$

where $\psi(R) = \frac{1}{D} \int_0^R \frac{dR}{\psi(R)}$ is the time-surface average value of bubble wall temperature gradient.

List of Symbols

a_z	thermal diffusivity
C	constant
c	specific heat
D	bubble diameters
D_0	bubble departure diameters corresponding to $\frac{dD}{dt} = 0$
f	bubble frequency
g	gravity acceleration
h_{fg}	latent heat of evaporation
k	thermal conductivity
q/A	heat flux
r^*	radius of nucleus
r	radius
R	bubble radius
t	time
T	temperature
T_s	saturation temperature
ΔT	temperature difference
v_{fg}	specific volume change on vaporization
β	contact angle
ρ	density
σ	surface tension
$\phi(R)$	surface average bubble wall temperature gradient
$\psi(R)$	surface-time average bubble wall temperature gradient
Subscripts	
l	liquid
v	vapor

References

1. Plesset, M. J. and Zwick, S. A., "Growth of Vapor Bubbles in Superheated Liquids", *Journal of Applied Physics* 25; 493-500 (1953).
2. Forster, H. K. and Zuber, N., "Growth of a Vapor Bubble in a Superheated Liquid", *Journal of Applied Physics* 24, 474-478 (1953).
3. Griffith, P., "Bubble Growth Rates in Boiling", *ASME Trans.* 80 721-722 (1958).
4. Bankoff, S. A. and Mikesell, R. D., "Growth of Bubbles in a Liquid of Initially Non-uniform Temperature", *ASME Paper* 58-A-105.
5. Zmola, P. C., "Investigation of the Mechanism of Boiling in Liquids", Ph.D. Thesis, Purdue University, W. Lafayette, Indiana, June 1950.
6. Ellion, M. "Study of the Mechanism of Boiling Heat Transfer", C.I.T., Pasadena, Calif., JPL Memo, 20-88, March 1954.
7. Gunther, F. C., "Photographic Study of Surface Boiling Heat Transfer to Water with Forced Convection", C.I.T., Pasadena, Calif., JPL Prog. Rep. 4-75, June 1950.
8. Mikesell, R. D., "Bubble Dynamics in Nucleate Boiling Heat Transfer", M.S. Thesis, Rose Polytechnic Institute, Terre Haute, Ind., June 1958.
9. Fritz, W., *Physikalische Zeitschrift*, Vol. 36, p. 379 (1935).
10. Jakob, M., "Heat Transfer", Vol. 1, p. 631-7, Wiley, New York 1949.

Figures

Figure 1 The general plan of experimental set-up

Figure 2 Section of boiling unit

Figure 3 The bubble diameter vs. time curves for water taken at atmospheric pressure with the heating surface horizontal

$$q/A = 8.10^4 \frac{\text{Btu}}{\text{hr ft}^2} \quad \Delta T = 21.6^\circ\text{F}$$

Figure 4 The bubble diameters vs. time curves for water at atmospheric pressure with the heating surface horizontal

$$q/A = 1.36 \cdot 10^5 \frac{\text{Btu}}{\text{hr ft}^2} \quad \Delta T = 25.7^\circ\text{F}$$

Figure 5 The bubble diameter vs. time curves for water at atmospheric pressure with the heating surface horizontal

Bubbles No. 1, No. 2 and No. 3: $q/A = 5.5 \cdot 10^4 \frac{\text{Btu}}{\text{hr ft}^2} \quad \Delta T = 15.3^\circ\text{F}$

Bubbles No. 4 and No. 5: $q/A = 2.1 \cdot 10^5 \frac{\text{Btu}}{\text{hr ft}^2} \quad \Delta T = 28.8^\circ\text{F}$

Figure 6 The bubble diameter vs. time curves for water at atmospheric pressure with the heating surface horizontal

Bubbles No. 1, No. 2, No. 3 and No. 4: $q/A = 7.5 \cdot 10^4 \frac{\text{Btu}}{\text{hr ft}^2} \quad \Delta T = 20.5^\circ\text{F}$

Bubbles No. 5 and No. 6: $q/A = 5.5 \cdot 10^4 \frac{\text{Btu}}{\text{hr ft}^2} \quad \Delta T = 15.1^\circ\text{F}$

Figure 7 The bubble diameter vs. time curves for water at atmospheric pressure with the heating surface horizontal

$$q/A = 2.94 \cdot 10^5 \frac{\text{Btu}}{\text{hr ft}^2} \quad \Delta T = 35^\circ\text{F}$$

Figure 8 The bubble diameters vs. time curves for water at atmospheric pressure with the small thickness of liquid layers above the heating surface

$$\text{Bubbles No. 1, No. 2 and No. 3: } q/A = 1.1 \cdot 10^5 \frac{\text{Btu}}{\text{hr ft}^2} \Delta T = 21.2^\circ\text{F}$$

$$\text{Bubbles No. 4 and No. 5: } q/A = 1.82 \cdot 10^5 \frac{\text{Btu}}{\text{hr ft}^2} \Delta T = 26.8^\circ\text{F}$$

Figure 9 The bubble diameter vs. time curves for water at the pressure 28 psi with the heating surface horizontal

$$q/A = 6.1 \cdot 10^4 \frac{\text{Btu}}{\text{hr ft}^2} \Delta T = 13.6^\circ\text{F}$$

Figure 10 The bubble diameters vs. time curves for water at the pressure 28 psi with the heating surface horizontal

$$\text{Bubbles No. 1, No. 2 and No. 3: } q/A = 5.7 \cdot 10^4 \frac{\text{Btu}}{\text{hr ft}^2} \Delta T = 12.2^\circ\text{F}$$

$$\text{Bubble No. 4: } q/A = 1.09 \cdot 10^5 \frac{\text{Btu}}{\text{hr ft}^2} \Delta T = 16^\circ\text{F}$$

Figure 11 The bubble diameter vs. time curves for water at the pressure 40 psi with the heating surface horizontal

$$q/A = 7.2 \cdot 10^4 \text{ Btu/hr ft}^2 \Delta T = 13^\circ\text{F}$$

Figure 12 The bubble diameter vs. time curve for water at atmospheric pressure, with the heating surface vertical

$$q/A = 9.4 \cdot 10^4 \text{ Btu/hr ft}^2 \Delta T = 19^\circ\text{F}$$

Figure 13 The bubble diameter vs. time curves for methyl alcohol at atmospheric pressure

$$\text{Bubbles No. 1 and No. 2: } q/A = 3.5 \cdot 10^4 \text{ Btu/hr ft}^2; \Delta T = 24.5^\circ\text{F}$$

$$\text{Bubbles No. 3 and No. 4: } q/A = 5.1 \cdot 10^4 \text{ Btu/hr ft}^2; \Delta T = 29.3^\circ\text{F}$$

$$\text{Bubble No. 5: } q/A = 7.9 \cdot 10^4 \text{ Btu/hr ft}^2; \Delta T = 34.2^\circ\text{F}$$

Figure 14 The bubble diameters vs. time curves for methyl alcohol

Bubbles No. 1 and 2: $p=28$ psi $q/A = 3.5 \cdot 10^4$ Btu/hr ft² $\Delta T = 17^\circ F$

Bubble No. 3: $p = 28$ psi $q/A = 3.6 \cdot 10^4$ Btu/hr ft² $\Delta T = 14.7^\circ F$

Bubble No. 4: $p = 40$ psi $q/A = 3.7 \cdot 10^4$ Btu/hr ft² $\Delta T = 13^\circ F$

Figure 15 The diameter of bubbles and frames number vs. time for a single active site observed during the longer time

Figure 16 The correlation of ratio D/D_0 versus the growth velocity in the last stage of growth

<u>Water:</u>	o	atmospheric pressure	$q/A = 8 \cdot 10^4$ Btu/hr ft ²
	x	"	$q/A = 1.36 \cdot 10^5$ Btu/hr ft ²
	▽	"	$q/A = 5.5 \cdot 10^4$ Btu/hr ft ²
	△	"	$q/A = 2.1 \cdot 10^5$ Btu/hr ft ²
	□	"	$q/A = 2.94 \cdot 10^5$ Btu/hr ft ²
	•	"	$q/A = 1.1 \cdot 10^5$ Btu/hr ft ²
	⊙	"	$q/A = 1.82 \cdot 10^5$ Btu/hr ft ²
	⊗	"	$q/A = 7.5 \cdot 10^4$ Btu/hr ft ²
	■	"	$q/A = 5.5 \cdot 10^4$ Btu/hr ft ²
	⊠	$p = 28$ psi	$q/A = 5.7 \cdot 10^4$ Btu/hr ft ²
	⊙	$p = 28$ psi	$q/A = 1.09 \cdot 10^5$ Btu/hr ft ²
	▲	$p = 28$ psi	$q/A = 6.1 \cdot 10^4$ Btu/hr ft ²
	⊙	$p = 40$ psi	$q/A = 7.2 \cdot 10^4$ Btu/hr ft ²

Methyl alcohol:

⊙	atmospheric pressure	$q/A = 3.5 \cdot 10^4$ Btu/hr ft ²
▽	"	$q/A = 7.9 \cdot 10^4$ Btu/hr ft ²
▲	"	$q/A = 5.1 \cdot 10^4$ Btu/hr ft ²
⊙	$p = 28$ psi	$q/A = 3.5 \cdot 10^4$ Btu/hr ft ²
⊠	$p = 28$ psi	$q/A = 3.6 \cdot 10^4$ Btu/hr ft ²
⊙	$p = 40$ psi	$q/A = 3.7 \cdot 10^4$ Btu/hr ft ²

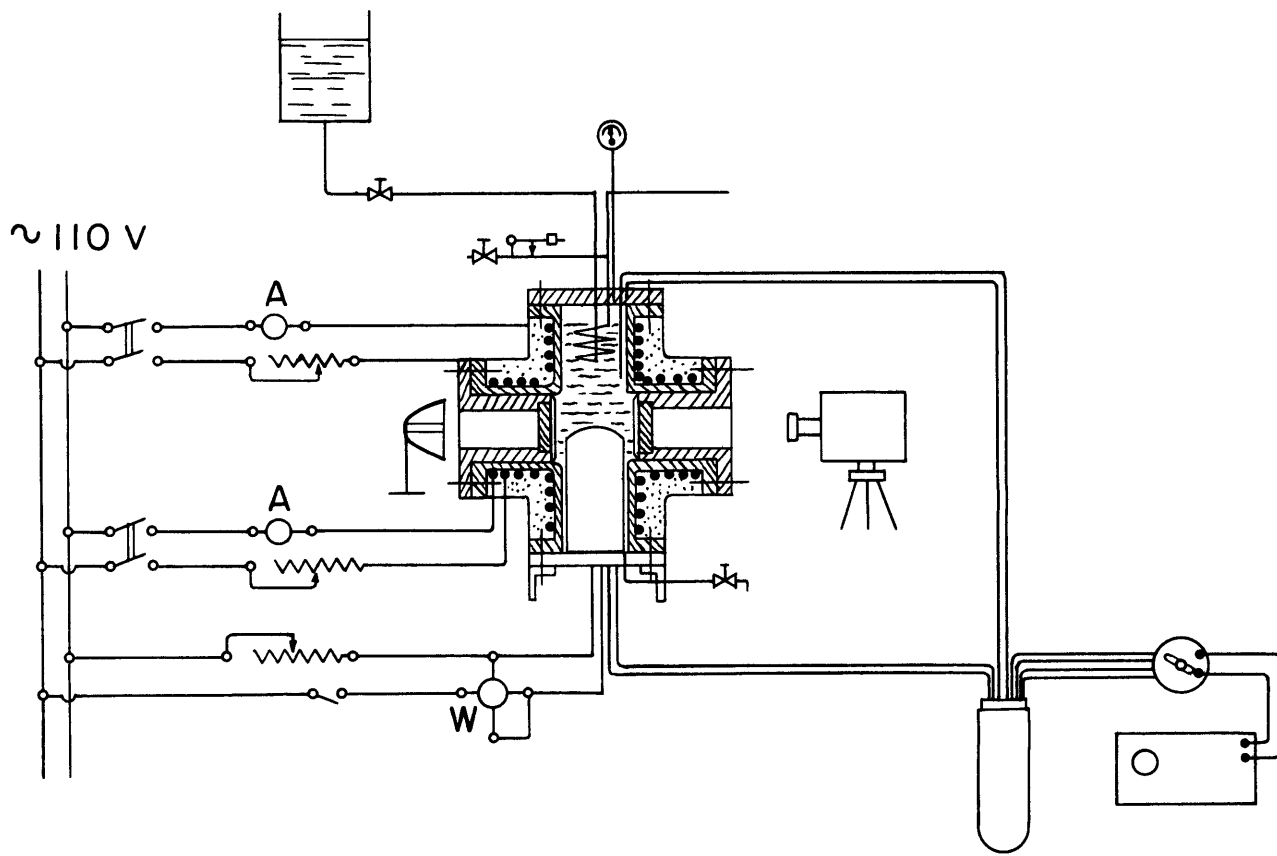


FIG. 1

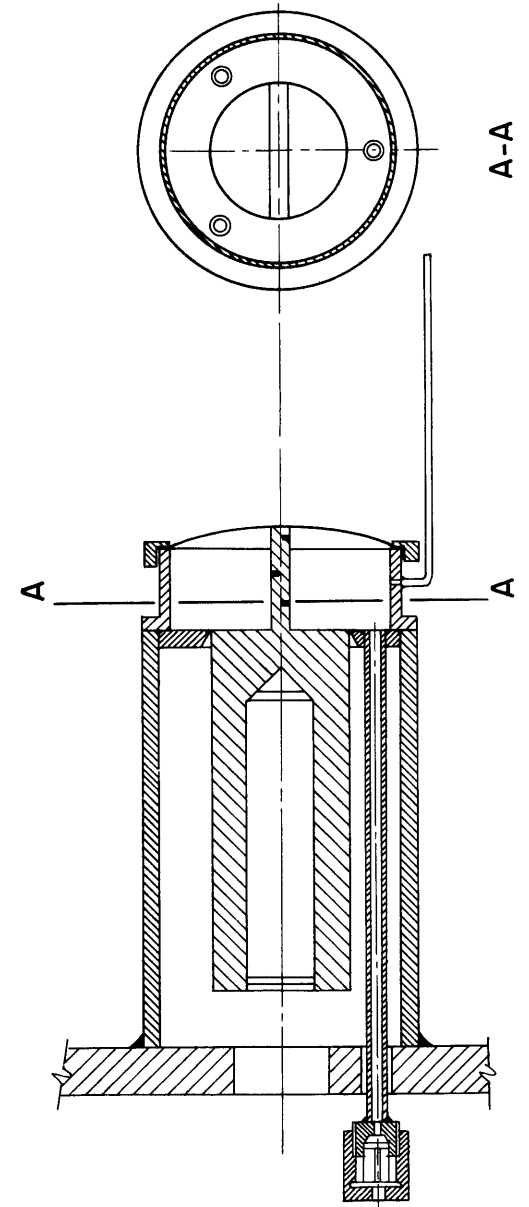


FIG. 2

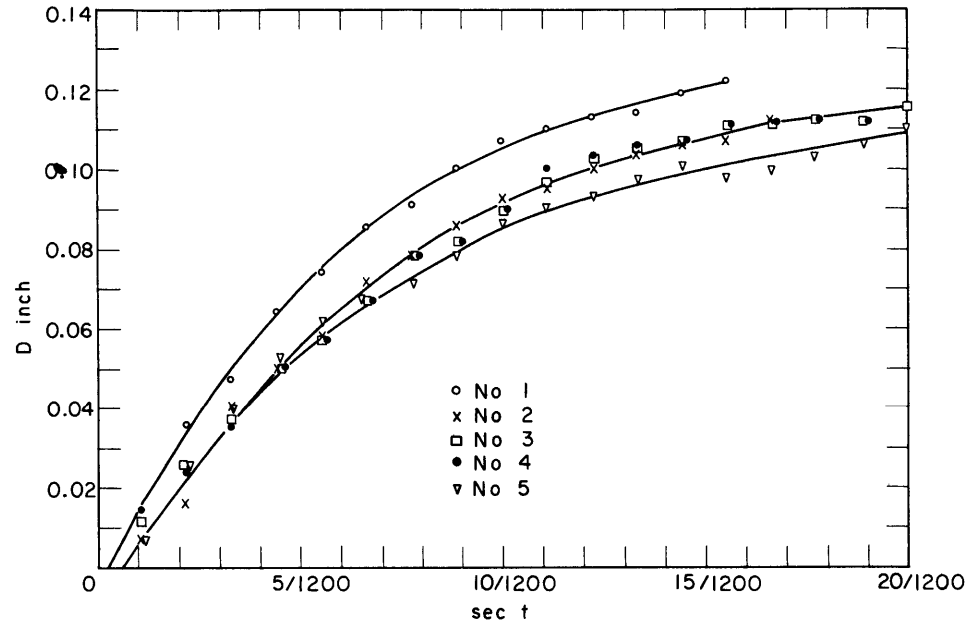


FIG. 3

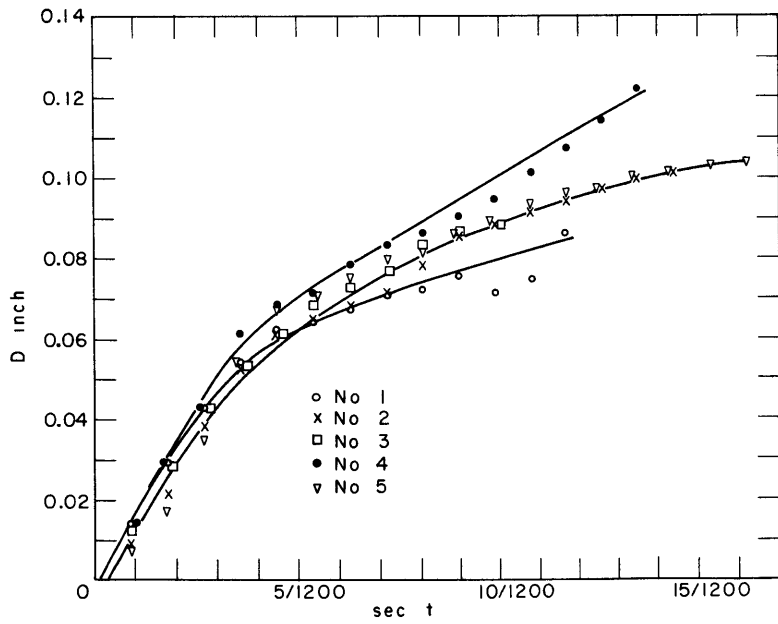


FIG. 4

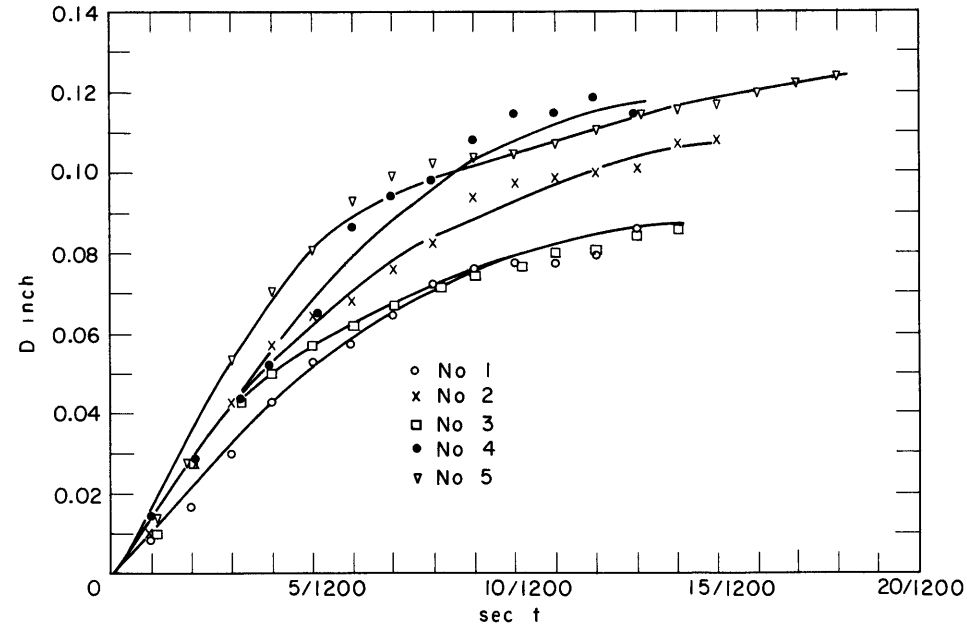


FIG. 5

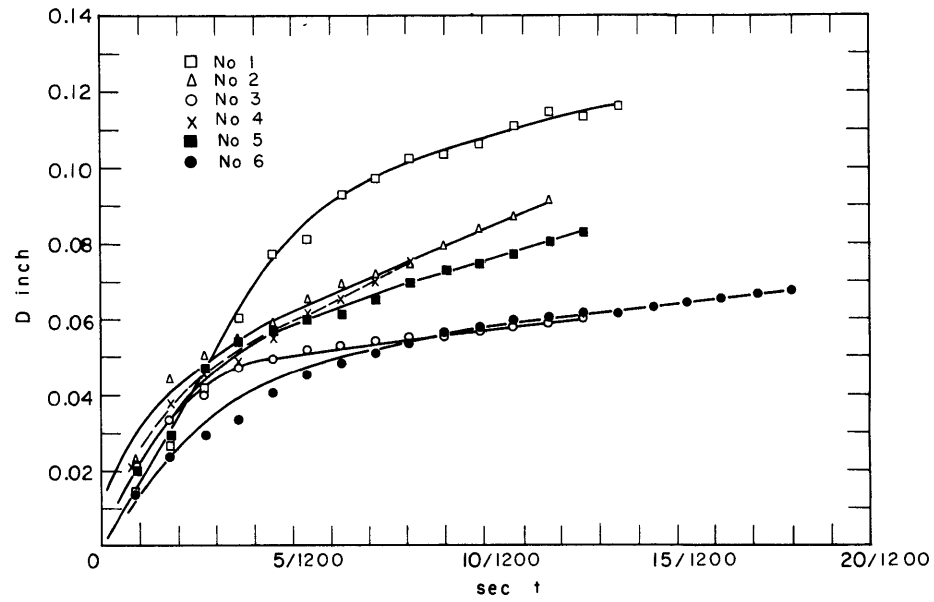


FIG. 6

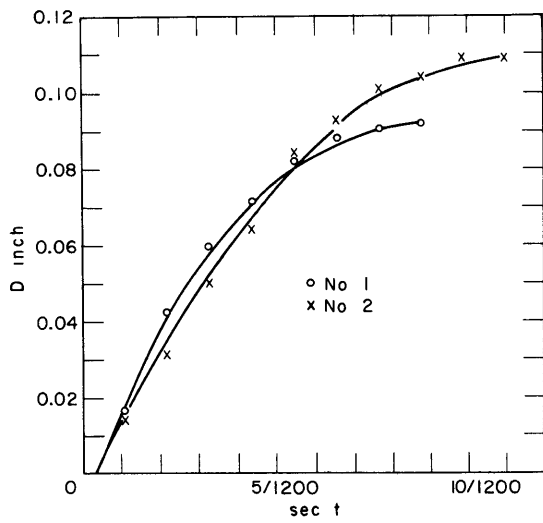


FIG. 7

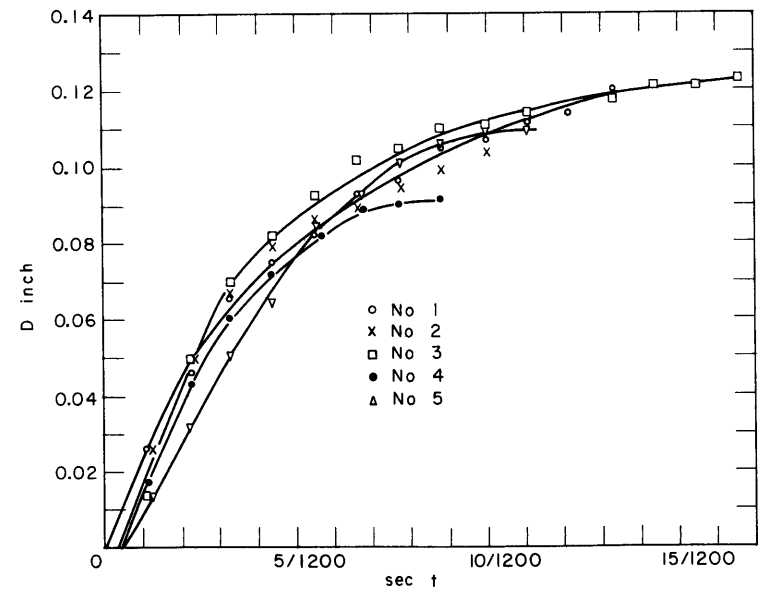


FIG. 8

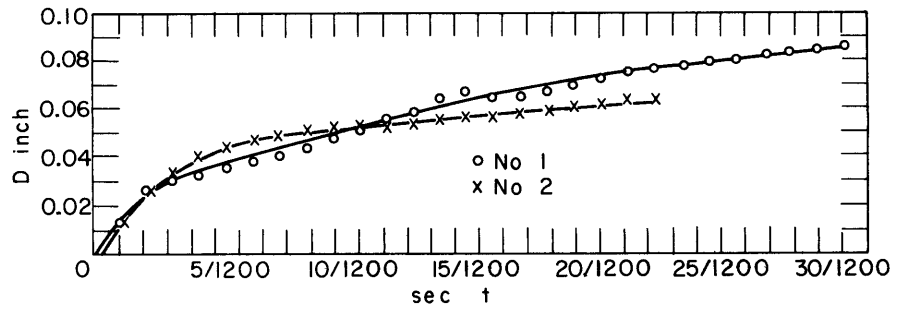


FIG. 9

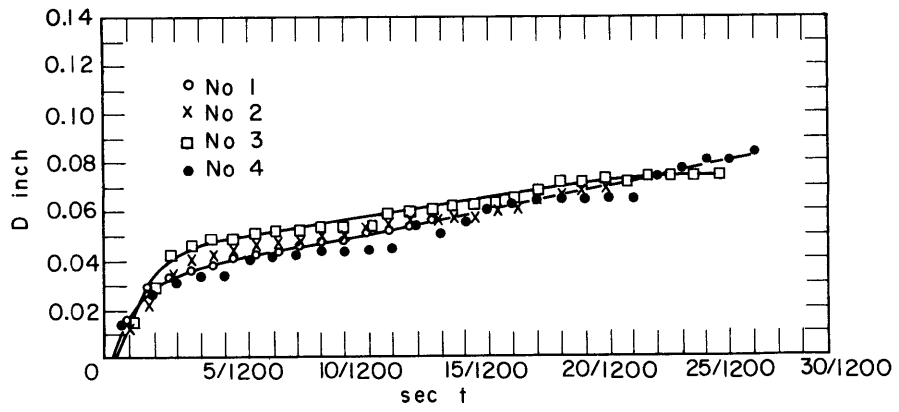


FIG. 10

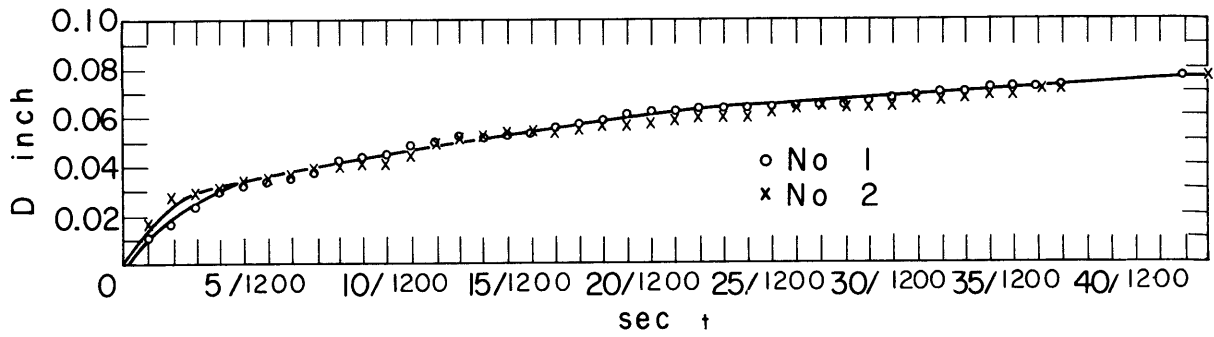


FIG. 11

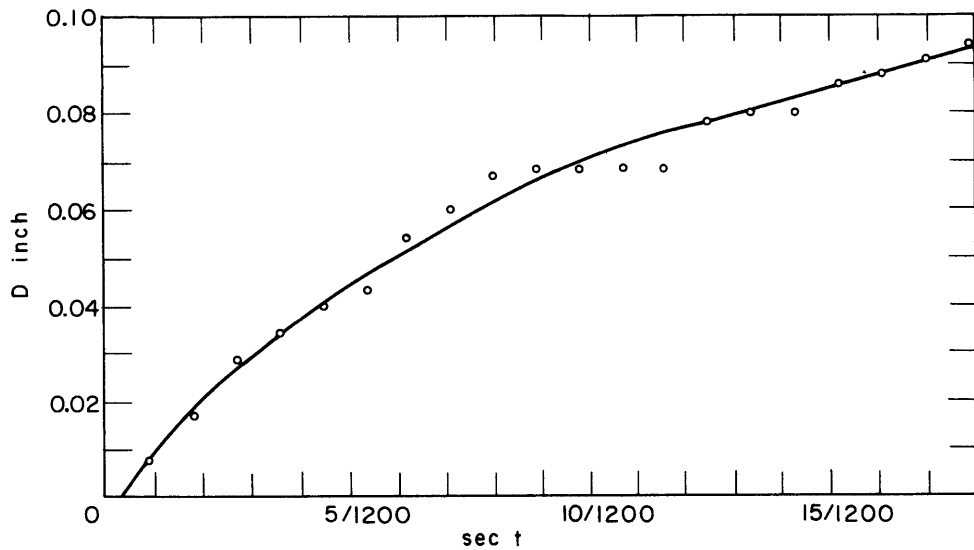


FIG. 12

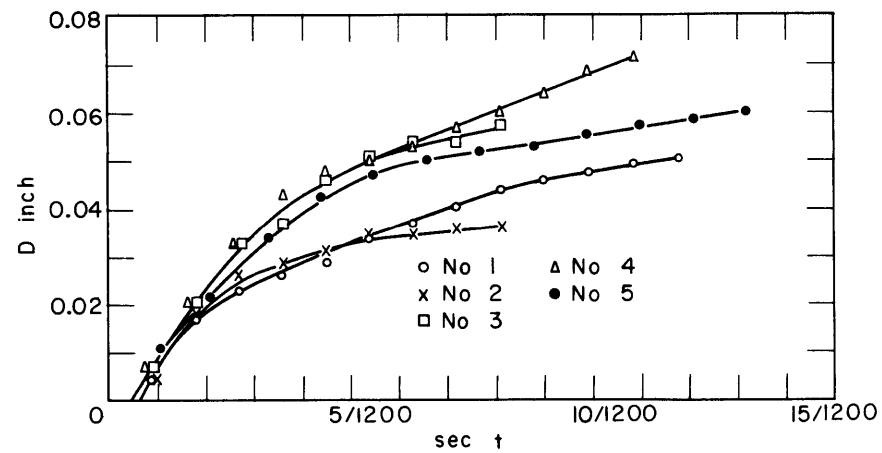


FIG. 13

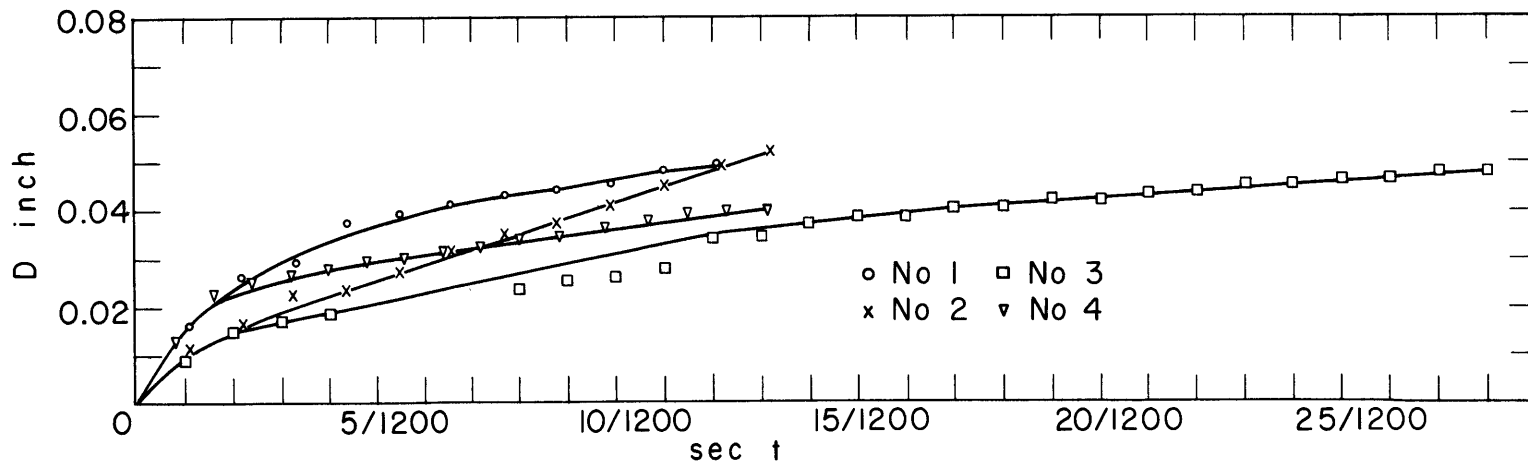


FIG. 14

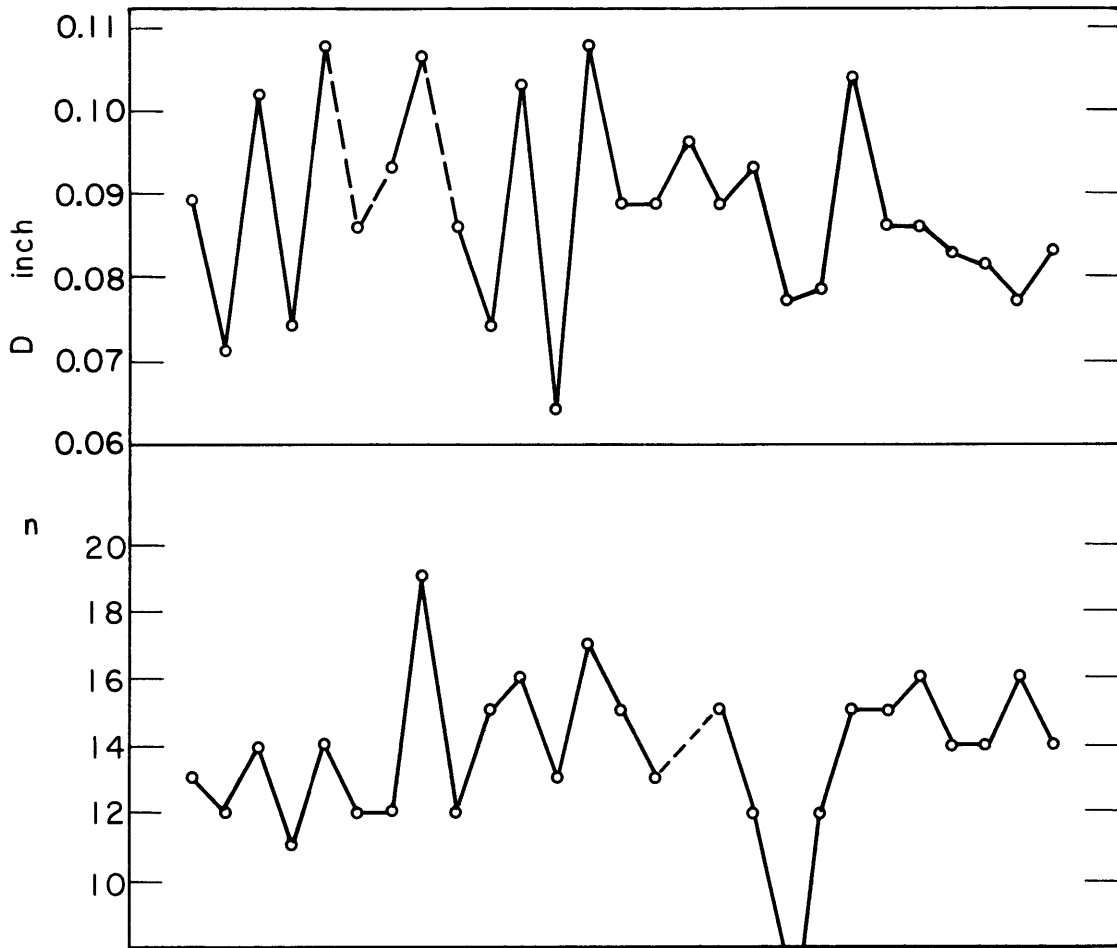


FIG. 15

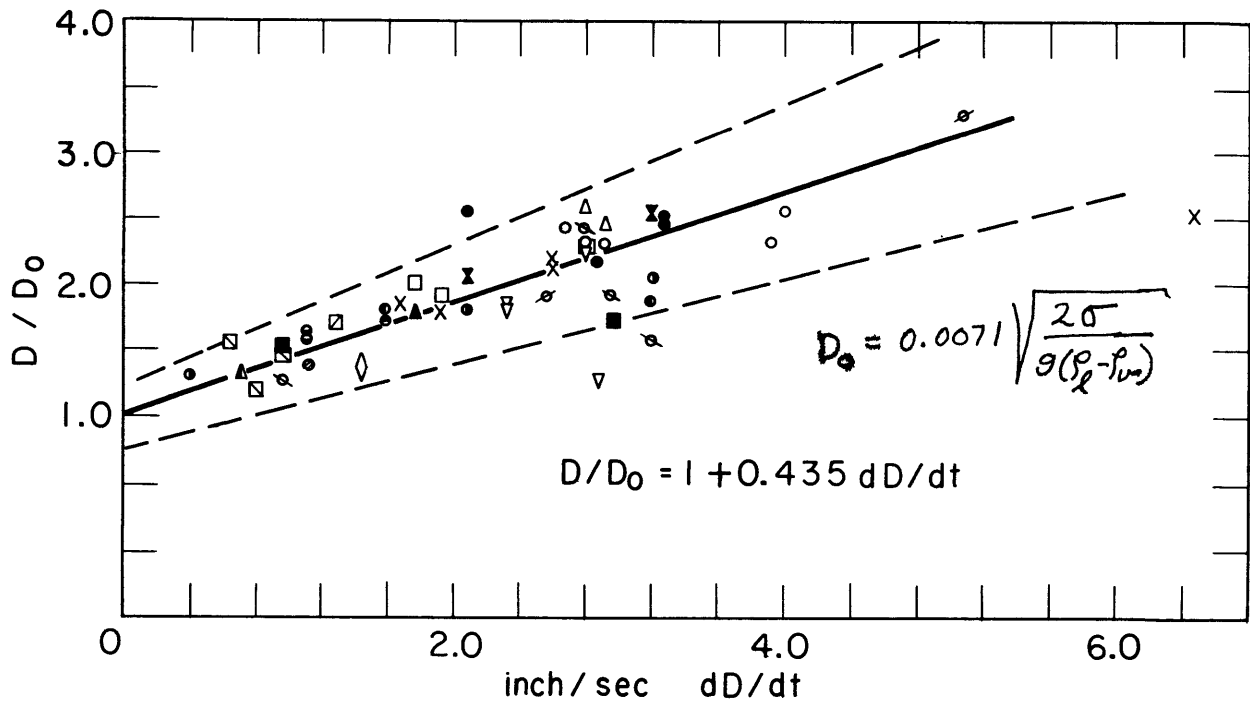


FIG. 16